

**Fluorine-substituted Mg(BH<sub>4</sub>)<sub>2</sub>•2NH<sub>3</sub> with improved dehydrogenation properties for hydrogen storage**

Journal:	<i>Journal of Materials Chemistry A</i>
Manuscript ID:	TA-ART-09-2014-004765.R1
Article Type:	Paper
Date Submitted by the Author:	15-Oct-2014
Complete List of Authors:	Yang, Yanjing; Zhejiang University, Department of Materials Science and Engineering Liu, Yongfeng; Zhejiang University, Department of Materials Science and Engineering Li, You; Zhejiang University, Department of Materials Science and Engineering Gao, Mingxia; Zhejiang University, Department of Materials Science and Engineering Pan, Hongge; Zhejiang University, Department of Materials Science and Engineering

## ARTICLE

# Fluorine-substituted $\text{Mg}(\text{BH}_4)_2 \cdot 2\text{NH}_3$ with improved dehydrogenation properties for hydrogen storage

Cite this: DOI: 10.1039/x0xx00000x

Yanjing Yang,<sup>a,b</sup> Yongfeng Liu,<sup>a\*</sup> You Li,<sup>a</sup> Mingxia Gao,<sup>a</sup> Hongge Pan<sup>a\*</sup>Received 00th January 2012,  
Accepted 00th January 2012

DOI: 10.1039/x0xx00000x

www.rsc.org/

The F-substituted  $\text{Mg}(\text{BH}_4)_2 \cdot 2\text{NH}_3$  was successfully prepared for the first time by mechanochemically reacting  $\text{Mg}(\text{BH}_4)_2 \cdot 2\text{NH}_3$  and  $\text{LiBF}_4$  based on the structural and chemical similarity of  $[\text{BH}_4]^-$  and  $[\text{BF}_4]^-$  anions. The results indicate that the dehydrogenation properties of  $\text{Mg}(\text{BH}_4)_2 \cdot 2\text{NH}_3$  are significantly improved by the partial substitution of fluorine for hydrogen. Hydrogen release from the F-substituted  $\text{Mg}(\text{BH}_4)_2 \cdot 2\text{NH}_3$  is initiated at approximately 70 °C, which is an 80 °C decrease in comparison with the pristine sample. At 150 °C, the 15 mol% F-substituted sample releases ~ 5.2 wt% of hydrogen within 40 min. However, only 1.2 wt% of hydrogen could be desorbed from the pristine  $\text{Mg}(\text{BH}_4)_2 \cdot 2\text{NH}_3$  under identical conditions. Mechanistic investigations reveal that the B-H bonds in  $\text{Mg}(\text{BH}_4)_2 \cdot 2\text{NH}_3$  are strengthened after F-substitution, which induces more ionised  $\text{H}^{\delta-}$  in the ammoniate and consequently facilitates the local  $\text{H}^{\delta+}$ - $\text{H}^{\delta-}$  combinations within the  $\text{Mg}(\text{BH}_4)_2 \cdot 2\text{NH}_3$  molecule. In addition, the F-substitution weakens the Mg-B bonds in  $\text{Mg}(\text{BH}_4)_2 \cdot 2\text{NH}_3$ , which favours the generation of B-N bonds during dehydrogenation. These factors are the most important reasons for the improved dehydrogenation properties of F-substituted  $\text{Mg}(\text{BH}_4)_2 \cdot 2\text{NH}_3$ .

## Introduction

Hydrogen is widely regarded as a green and alternative source of energy.<sup>1,2</sup> However, the lack of safe, efficient and economical hydrogen-storage technologies hinders its practical applications, especially in proton exchange membrane fuel cells (PEMFCs). Compared with traditional compressed gas and liquefied hydrogen storage, storing hydrogen in solid materials results in considerably safer operating conditions and higher volumetric capacities, making storage in solid materials a more favourable storage technology and thus the focus of the present investigation.<sup>3</sup> Among the solid materials developed for hydrogen storage, metal borohydrides containing  $[\text{BH}_4]^-$  anions have been attracting great interest because of their high gravimetric hydrogen capacity.<sup>4</sup> Unfortunately, metal borohydrides as hydrogen storage materials suffer from high thermal stability, slow dehydrogenation/hydrogenation kinetics and poor reversibility.<sup>4,5</sup> Extensive work has been done to address these thermodynamic and kinetic limitations, including catalyst doping,<sup>6,7</sup> reactive composites,<sup>8,9</sup> size-modification<sup>10,11</sup> and cation-/anion-substitution,<sup>12,13</sup> etc. However, none of the borohydride-based systems developed to date can satisfy all the requirements for practical hydrogen-storage materials.

Recently, several promising hydrogen-storage systems involving the combination of  $\text{H}^{\delta+}$ - $\text{H}^{\delta-}$  during dehydrogenation

were discovered to possess good hydrogen storage properties. These hydrogen-storage systems include ammonia borane (AB),<sup>14,15</sup> metal amidoboranes (MABs),<sup>16,17</sup> and amide-hydride.<sup>18-22</sup> In addition, the formation of metal borohydride ammoniates by adducting  $\text{NH}_3$  groups to metal borohydrides also creates an environment of local  $\text{H}^{\delta+}$ - $\text{H}^{\delta-}$  coexistence, thereby possessing dehydrogenation properties superior to the corresponding metal borohydrides.<sup>23-27</sup>

Magnesium borohydride diammoniate ( $\text{Mg}(\text{BH}_4)_2 \cdot 2\text{NH}_3$ ), which has a gravimetric hydrogen capacity as high as 16.03 wt% and a low dehydrogenation temperature of approximately 150 °C, has considerable potential as a practical hydrogen storage material for PEMFCs.<sup>25,26</sup> However, the hydrogen released from this ammoniate suffers from contamination by ammonia, which is a poison for PEMFCs.<sup>26</sup> In addition, the dehydrogenation temperature is still too high for practical applications. Considerable work has been conducted to improve the dehydrogenation properties of metal borohydride ammoniates by changing the coordination number of  $\text{NH}_3$  or forming mixed-cation borohydride ammoniates for hydrogen storage.<sup>26-28</sup> Recently, we investigated  $\text{Mg}(\text{BH}_4)_2 \cdot x\text{NH}_3$  ( $x=1, 2, 3, 6$ ) as hydrogen storage materials and discovered the close correlation between the dehydrogenation properties and the coordination numbers of  $\text{NH}_3$ .<sup>26</sup> In addition, several mixed-cation borohydride ammoniates, including  $\text{LiMg}(\text{BH}_4)_3 \cdot 2\text{NH}_3$ ,

$\text{Li}_2\text{Mg}(\text{BH}_4)_4 \cdot 3\text{NH}_3$ ,  $\text{Li}_2\text{Mg}(\text{BH}_4)_2 \cdot 6\text{NH}_3$  and  $\text{Li}_2\text{Al}(\text{BH}_4)_5 \cdot 6\text{NH}_3$  have been discovered to possess dehydrogenation properties superior to the corresponding monometallic  $\text{Mg}(\text{BH}_4)_2 \cdot 2\text{NH}_3$ ,  $\text{Mg}(\text{BH}_4)_2 \cdot 3\text{NH}_3$ ,  $\text{Mg}(\text{BH}_4)_2 \cdot 6\text{NH}_3$  and  $\text{Al}(\text{BH}_4)_3 \cdot 6\text{NH}_3$ , respectively.<sup>23,27,28</sup>

More interestingly, previous studies demonstrated that  $\text{TiF}_3$  is notably superior to  $\text{TiCl}_3$  in improving the hydrogen storage properties of  $\text{LiBH}_4$ . This superiority is attributed to the possible substitution of fluorine for hydrogen in  $\text{LiBH}_4$  and  $\text{LiH}$  to generate  $\text{LiBH}_{4-x}\text{F}_x$  and  $\text{LiH}_{1-x}\text{F}_x$ , respectively, during dehydrogenation.<sup>6,29,30</sup> Further density functional theory (DFT) calculations revealed a linear reduction in the enthalpy change of the decomposition of  $\text{Li}_8\text{B}_8\text{H}_{32-x}\text{F}_x$  with increasing the substitution level from  $x = 1$  to  $x = 4$ .<sup>31</sup> These results suggest the feasibility of tuning the hydrogen-storage properties of metal borohydride-related materials through the substitution of fluorine for hydrogen in  $[\text{BH}_4]^-$  anions. However, a key challenge is how to successfully introduce F into the  $[\text{BH}_4]^-$  groups. As early as the 1950s and 1960s, Brown et al. proposed a synthetic route to  $\text{MBHX}_3$  compounds via the reaction between  $\text{MH}$  and  $\text{BX}_3$  (M: metal, X: halide).<sup>32,33</sup> In 1961,  $\text{KBH}_3\text{F}$  was successfully obtained by Aftandilian et al. through the reaction of  $\text{KF}$  and  $\text{B}_2\text{H}_6$ .<sup>34</sup> More inspiringly, the theoretical calculation indicated that F-substitution in  $\text{LiBH}_4$  was more thermodynamically favourable than the formation of  $\text{LiB}(\text{H},\text{F})_4$  solid solutions when mixing  $\text{LiBH}_4$  and  $\text{LiBF}_4$ .<sup>30</sup> Therefore, taking into consideration the similarity in chemical properties and ionic sizes between the  $[\text{BF}_4]^-$  anion (2.4 Å) and  $[\text{BH}_4]^-$  anion (2.03 Å),<sup>35</sup> as well as the  $\text{F}^-$  anion (1.33 Å) and  $\text{H}^-$  anion (1.47 Å),<sup>36</sup> we believe that it is feasible to partially substitute hydrogen in a  $[\text{BH}_4]^-$  anion with fluorine by interacting metal borohydrides and borofluorides. Such a conjecture was preliminarily validated by Heyn et al., who reported the formation of potassium fluoroborohydrides  $\text{K}(\text{BH}_x\text{F}_{4-x})$  ( $x = 0-4$ ) by reacting  $\text{KBH}_4$  and  $\text{KBF}_4$ .<sup>37</sup> In addition, the hydrogen-fluorine exchange in the  $\text{NaBH}_4$ - $\text{NaBF}_4$  systems also induced the formation of fluorine-substituted sodium borohydride  $\text{NaBH}_2\text{F}_2$ , which exhibits a lower decomposition temperature in comparison with the pristine  $\text{NaBH}_4$ .<sup>38</sup>

In this work, to achieve the manipulation of the intrinsic dehydrogenation thermodynamics of  $\text{Mg}(\text{BH}_4)_2 \cdot 2\text{NH}_3$ , lithium borofluoride ( $\text{LiBF}_4$ ) was employed as the fluorine source and an F-substituted  $\text{Mg}(\text{BH}_4)_2 \cdot 2\text{NH}_3$  was successfully prepared for the first time through the mechanochemical reaction of  $\text{Mg}(\text{BH}_4)_2 \cdot 2\text{NH}_3$  and  $\text{LiBF}_4$ . The effects of F-substitution on the dehydrogenation properties of  $\text{Mg}(\text{BH}_4)_2 \cdot 2\text{NH}_3$  and the corresponding mechanisms were systematically studied and elucidated.

## Experimental Section

### Materials and Sample Preparation

The commercially available chemicals, sodium borohydride ( $\text{NaBH}_4$ , Alfa Aesar, 98%), anhydrous magnesium chloride ( $\text{MgCl}_2$ , Alfa Aesar, 99%), lithium borohydride ( $\text{LiBH}_4$ , Sigma

Aldrich, 95%), lithium borofluoride ( $\text{LiBF}_4$ , Sigma-Aldrich, 99.99%), and magnesium fluoride ( $\text{MgF}_2$ , Alfa Aesar, 99%) were purchased and used as received. Anhydrous diethyl ether was delivered from Sinopharm Chemical and further dried with calcium hydride ( $\text{CaH}_2$ ). Anhydrous ammonia gas ( $\text{NH}_3$ ) was also used as received. Magnesium borohydride ( $\text{Mg}(\text{BH}_4)_2$ , 96%) was synthesised via the metathesis reaction between sodium borohydride and magnesium chloride in diethyl ether as described in our previous report.<sup>39</sup> Magnesium borohydride hexaammoniate ( $\text{Mg}(\text{BH}_4)_2 \cdot 6\text{NH}_3$ ) was obtained by ball milling  $\text{Mg}(\text{BH}_4)_2$  under 6 bar of an ammonia atmosphere, and  $\text{Mg}(\text{BH}_4)_2 \cdot 2\text{NH}_3$  was prepared by ball milling the mixture of  $\text{Mg}(\text{BH}_4)_2 \cdot 6\text{NH}_3$  and  $\text{Mg}(\text{BH}_4)_2$  with a molar ratio of 1:2 in an Ar atmosphere.<sup>26</sup> The F-substituted  $\text{Mg}(\text{BH}_4)_2 \cdot 2\text{NH}_3$  samples with different substitutions (expressed by the  $\text{F}^{\delta-}/(\text{F}^{\delta-} + \text{H}^{\delta-})$  ratios) of 2.5, 5, 10, 15, 20 and 25 mol% were prepared via ball milling the corresponding chemicals on a planetary ball mill (QM-3SP4) rotating at 500 rpm for 3 h. A gas valve that can be connected to a pressure gauge for measuring the inside pressure was mounted on the cover of the milling jar. To ensure even mixing and milling and to limit the temperature rise during milling, the mill was set to rotate for 0.2 h in one direction, followed by a pause of 0.1 h and subsequent rotation in the reverse direction. No obvious temperature rise was observed owing to the ventilation device inside the compartment of the mill.

### Structural Characterisation

Phase identification was conducted using powder X-ray diffraction (XRD) on a Phillips X'Pert Pro X-ray Diffractometer with  $\text{Cu K}\alpha$  radiation at 40 kV and 40 mA. Data were collected from  $10^\circ$  to  $90^\circ$  ( $2\theta$ ) with step increments of  $0.02^\circ$  at ambient temperature. A specially designed sample container was adapted to protect samples from contamination from the oxygen and moisture during sample transfer and testing.

Vibrational characteristics of the B-H and N-H bonds were determined by a Bruker Tensor 27 Fourier Transform Infrared (FTIR) spectrometer. The FTIR spectra of all the samples (as KBr pellets with a KBr-to-sample weight ratio of approximately 100:1) were acquired in the range of  $4000-400 \text{ cm}^{-1}$ , and the transmission mode was adopted with a resolution of  $4 \text{ cm}^{-1}$ .

### Property Evaluation

Temperature-programmed desorption (TPD) measurements were performed on a custom-designed apparatus attached with an online mass spectrometer (MS, Hiden QIC-20). Approximately 40 mg of sample was loaded into a specially designed tube reactor that allows the purge argon gas to get through upon heating. The temperature of the reactor was gradually elevated from room temperature to  $600^\circ\text{C}$  at a ramping rate of  $2^\circ\text{C min}^{-1}$ .

Quantitative hydrogen desorption behaviour of the F-substituted  $\text{Mg}(\text{BH}_4)_2 \cdot 2\text{NH}_3$  samples was evaluated with a custom-designed Sieverts-type apparatus. Typically,

approximately 80 mg of sample was loaded into a stainless steel reactor in the glove box and then connected to the Sieverts-type apparatus. After evacuating the system to  $10^{-3}$  bar, the sample was heated to a desired temperature at  $2\text{ }^{\circ}\text{C min}^{-1}$  (initially in vacuum). The pressure and temperature data were recorded automatically. The amounts of hydrogen desorbed were calculated according to the pressure change in the system using the equation of state.

Differential scanning calorimetry (DSC) was conducted to determine the heat flow under a gas flow of  $50\text{ ml Ar min}^{-1}$  using a Netzsch DSC 200 F3 thermal analyser. Approximately 2-3 mg of sample was loaded into an Al crucible covered by a lid. The crucible was then put into the equipment and heated from room temperature to  $600\text{ }^{\circ}\text{C}$  at  $10\text{ }^{\circ}\text{C min}^{-1}$ .

## Results and Discussion

Six F-substituted  $\text{Mg}(\text{BH}_4)_2 \cdot 2\text{NH}_3$  samples with the molar ratios for  $\text{F}^{\delta-}/(\text{F}^{\delta-} + \text{H}^{\delta-})$  (F-substitution contents) of 2.5, 5, 10, 15, 20 and 25 mol% were prepared by ball milling the corresponding mixtures of  $\text{Mg}(\text{BH}_4)_2 \cdot 2\text{NH}_3$  and  $\text{LiBF}_4$ . After the ball-milling treatment, pressure increases were detected for the F-substituted  $\text{Mg}(\text{BH}_4)_2 \cdot 2\text{NH}_3$ , indicating the occurrence of gas release caused by the reactions between  $\text{Mg}(\text{BH}_4)_2 \cdot 2\text{NH}_3$  and  $\text{LiBF}_4$ . Only hydrogen was detected by means of MS in the gas released during ball milling. According to the equation of state, the hydrogen desorption amounts were calculated to be 0.137, 0.19, 0.25, 0.36, 0.53 and 0.66 wt% for the composites with the  $\text{F}^{\delta-}/(\text{F}^{\delta-} + \text{H}^{\delta-})$  molar ratios of 2.5, 5, 10, 15, 20 and 25 mol%, respectively. However, further increasing the F-substitution to 50 and 75 mol% induces a severe decrease in the stability of  $\text{Mg}(\text{BH}_4)_2 \cdot 2\text{NH}_3$  because nearly all of the hydrogen in the  $\text{Mg}(\text{BH}_4)_2 \cdot 2\text{NH}_3$  was evolved after ball milling (4.30 wt% hydrogen for 50 mol% F-substitution, and 2.06 wt% hydrogen for 70 mol% F-substitution), which is rather unfavourable for practical hydrogen-storage applications.

The as-prepared  $\text{Mg}(\text{BH}_4)_2 \cdot 2\text{NH}_3\text{-LiBF}_4$  composites as well as the pristine  $\text{Mg}(\text{BH}_4)_2 \cdot 2\text{NH}_3$  and  $\text{LiBF}_4$  treated under the same conditions were first subjected to XRD measurements. As shown in Fig. 1, both the post-milled  $\text{Mg}(\text{BH}_4)_2 \cdot 2\text{NH}_3$  and  $\text{LiBF}_4$  exhibit sharp diffraction peaks, indicating their good crystallinity. For the  $\text{Mg}(\text{BH}_4)_2 \cdot 2\text{NH}_3\text{-LiBF}_4$  composites with 2.5 and 5 mol% fluorine,  $\text{Mg}(\text{BH}_4)_2 \cdot 2\text{NH}_3$  was the only phase detected by XRD although their peak intensities were distinctly decreased. However,  $\text{LiBF}_4$  was invisible in these two samples, possibly due to its low content and/or the consumption during ball milling. As the F content was increased to 10 mol%, only the strongest diffraction peak of  $\text{Mg}(\text{BH}_4)_2 \cdot 2\text{NH}_3$  at  $16.9^{\circ}$  ( $2\theta$ ) could be detected. At the same time, a new diffraction peak at  $22.7^{\circ}$  ( $2\theta$ ) was also observed. Increasing the F content to 15 and 20 mol% led to the complete amorphisation of the corresponding  $\text{Mg}(\text{BH}_4)_2 \cdot 2\text{NH}_3\text{-LiBF}_4$  composites because no apparent diffraction peaks were observed in the XRD profiles. Upon further increasing the F content to 25 mol%, several broad and weak peaks of  $\text{MgF}_2$  could be identified at  $27.3$ ,  $40.4$ ,  $53.5$ , and  $68.2^{\circ}$  ( $2\theta$ ). In addition, a series of new peaks

emerged at  $20.2$ ,  $24.0$  and  $24.5^{\circ}$  ( $2\theta$ ), which could not be assigned to any known phases. Therefore, we speculate that a novel F-containing ammoniate may be formed through mechanochemically reacting  $\text{Mg}(\text{BH}_4)_2 \cdot 2\text{NH}_3$  with  $\text{LiBF}_4$ . Specifically, for the  $\text{Mg}(\text{BH}_4)_2 \cdot 2\text{NH}_3\text{-LiBF}_4$  composite with a  $\text{F}^{\delta-}/(\text{F}^{\delta-} + \text{H}^{\delta-})$  molar ratio of 25 mol%, the nominal composition of the product can be described as  $\text{MgLi}_{2/3}(\text{BH}_3\text{F})_{8/3} \cdot 2\text{NH}_3$ .

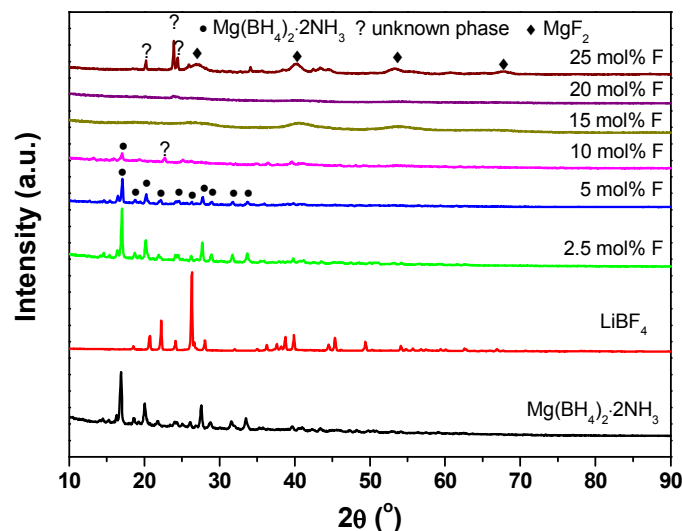


Fig. 1 XRD patterns of the post-milled  $\text{Mg}(\text{BH}_4)_2 \cdot 2\text{NH}_3\text{-LiBF}_4$  mixtures with different fluorine content.

Further FTIR examinations were conducted to identify the B-H and N-H bonds in the pristine  $\text{Mg}(\text{BH}_4)_2 \cdot 2\text{NH}_3$  and post-milled  $\text{Mg}(\text{BH}_4)_2 \cdot 2\text{NH}_3\text{-LiBF}_4$  composites. The results are shown in Fig. 2. There were clearly eight absorption bands detected in the FTIR spectrum of the pristine  $\text{Mg}(\text{BH}_4)_2 \cdot 2\text{NH}_3$ . The absorbance bands at  $3357$ ,  $3277$  and  $3215\text{ cm}^{-1}$  could be assigned to the N-H stretching modes, and those at  $2355$ ,  $2269$  and  $2193\text{ cm}^{-1}$  belong to three B-H stretching modes. Lastly, those at  $1234$  and  $1108\text{ cm}^{-1}$  are attributed to B-H bending modes.<sup>40</sup> After introducing 2.5 mol% fluorine, no obvious changes were detected for the B-H and N-H bonds of  $\text{Mg}(\text{BH}_4)_2 \cdot 2\text{NH}_3$ . In particular, when the F content was increased to 5 mol%, a blue shift was observed for the B-H stretching mode from  $2269$  to  $2273\text{ cm}^{-1}$ , which is possibly due to the substitution of F for H in the  $[\text{BH}_4]^-$  anions, although the B-H bending and N-H stretching modes remain unchanged. Further increasing the fluorine content to 10 mol% induced an additional blue shift to  $2288\text{ cm}^{-1}$  for the B-H stretching mode. Such a blue shift in the B-H stretching modes indicates the strengthening of the B-H bonding. In addition, two new B-H stretching absorbance modes at  $2224$  and  $2342\text{ cm}^{-1}$  were also detected, further confirming the alteration in the chemical environment of B and H upon fluorine substitution. These observations suggest that there is an interaction between the  $[\text{BF}_4]^-$  and  $[\text{BH}_4]^-$  anions, which possibly results in the formation of a novel F-substituted borohydride ammoniate. As for the 20 and 25 mol% fluorine-substituted  $\text{Mg}(\text{BH}_4)_2 \cdot 2\text{NH}_3$ , an appreciable change in the N-H bonds was observed as three

new N-H bands at 3254, 3278 and 3316  $\text{cm}^{-1}$  appeared. In addition, a new B-H stretching band at 2448  $\text{cm}^{-1}$  originating from the  $[\text{B}_{12}\text{H}_{12}]^{2-}$  anions<sup>41</sup> and a B-N band at 1383  $\text{cm}^{-1}$  were also discernible. These findings indicate that the newly formed fluorine-substituted  $\text{Mg}(\text{BH}_4)_2 \cdot 2\text{NH}_3$  may partially decompose during ball milling, which matches well with the pressure increase mentioned above. The occurrence of partial decomposition represents a significant decrease in the stability of the fluorine-substituted magnesium borohydride diammoniate. Moreover, the main B-F absorbance of the F-substituted  $\text{Mg}(\text{BH}_4)_2 \cdot 2\text{NH}_3$  was observed at 1064  $\text{cm}^{-1}$  in the FTIR spectra of the 20 and 25 mol% F-substituted samples, exhibiting a 6  $\text{cm}^{-1}$  blue shift relative to the pristine  $\text{LiBF}_4$  (1058  $\text{cm}^{-1}$ ). However, for the 5, 10 and 15 mol% F-substituted  $\text{Mg}(\text{BH}_4)_2 \cdot 2\text{NH}_3$  samples, only a shoulder was detected at the same position, possibly due to their lower fluorine content. Further investigations into the F-substitution mechanism revealed that there was no obvious change in the B-H and N-H bonds when mixing  $\text{Mg}(\text{BH}_4)_2$  and  $\text{MgF}_2$  through a procedure identical to the procedure applied to the  $\text{Mg}(\text{BH}_4)_2 \cdot 2\text{NH}_3$ - $\text{LiBF}_4$  composites (Fig. S1†). More importantly, no B-F bonds were detected in all the  $\text{Mg}(\text{BH}_4)_2 \cdot 2\text{NH}_3$ - $\text{MgF}_2$  systems. These results reveal that the  $[\text{BH}_4]^-$  anions and  $\text{NH}_3$  groups retain their integrity in the  $\text{Mg}(\text{BH}_4)_2 \cdot 2\text{NH}_3$ - $\text{MgF}_2$  systems. In other words, no chemical reactions took place between  $\text{MgF}_2$  and  $\text{Mg}(\text{BH}_4)_2 \cdot 2\text{NH}_3$ . Therefore, we deduce that the successful substitution of H in  $[\text{BH}_4]^-$  with F from  $[\text{BF}_4]^-$  can be attributed primarily to the similarity in chemical properties and ionic radii between the  $[\text{BH}_4]^-$  anion and  $[\text{BF}_4]^-$  anion, as well as the  $\text{F}^-$  anion and  $\text{H}^-$  anion.

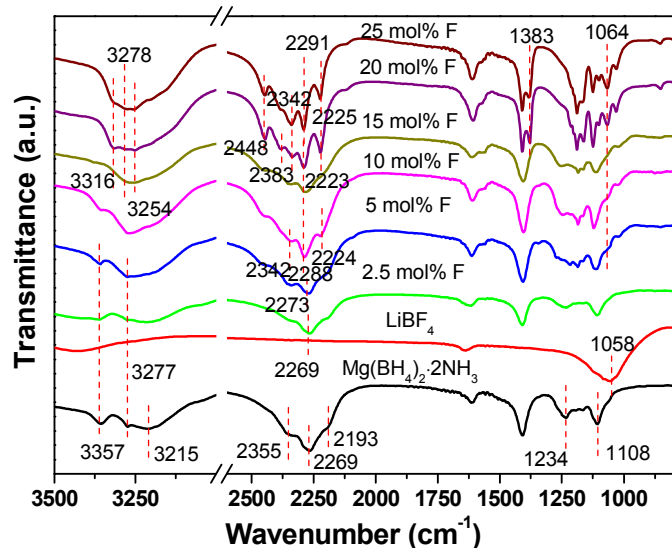


Fig. 2. FTIR spectra of the post-milled  $\text{Mg}(\text{BH}_4)_2 \cdot 2\text{NH}_3$ - $\text{LiBF}_4$  with different fluorine content.

Fig. 3 shows the TPD-MS curves of the post-milled F-substituted  $\text{Mg}(\text{BH}_4)_2 \cdot 2\text{NH}_3$ . Both the pristine and F-substituted  $\text{Mg}(\text{BH}_4)_2 \cdot 2\text{NH}_3$  present a stepwise thermal decomposition process. For the pristine  $\text{Mg}(\text{BH}_4)_2 \cdot 2\text{NH}_3$ , the  $\text{NH}_3$  was detected

at 105–225  $^\circ\text{C}$  upon decomposition, and hydrogen release began at 150  $^\circ\text{C}$  and peaked at 218 and 402  $^\circ\text{C}$ . After 2.5 mol% F-substitution, the  $\text{NH}_3$  release was completely depressed, which is very favourable for its practical applications in FEMFCs. Moreover, the onset dehydrogenation temperature was significantly reduced to 90  $^\circ\text{C}$ , representing a 60  $^\circ\text{C}$  reduction in comparison with the pristine  $\text{Mg}(\text{BH}_4)_2 \cdot 2\text{NH}_3$ . However, except for this subtle hydrogen-release process, the two main hydrogen-release processes were still found to exist between 150 to 300 and 400 to 500  $^\circ\text{C}$ . As for the 5 mol% F-substituted  $\text{Mg}(\text{BH}_4)_2 \cdot 2\text{NH}_3$ , an additional broad dehydrogenation peak was observed at 75–140  $^\circ\text{C}$ . With further increase in the F-substitution content, the dehydrogenation process at 75–140  $^\circ\text{C}$  was split into two peaks. The corresponding peaks were gradually broadened, and their intensities were increased. In particular, the dehydrogenation process at 75–165  $^\circ\text{C}$  dominated the TPD-MS curve, and those peaks at higher temperatures are nearly invisible when the F-substitution content was higher than 15 mol%. Only two overlapping dehydrogenation peaks were detected at 104 and 156  $^\circ\text{C}$  for the 25 mol% F-substituted sample. The thermal decomposition behaviour of  $\text{Mg}(\text{BH}_4)_2 \cdot 2\text{NH}_3$  was clearly changed with the presence of fluorine.

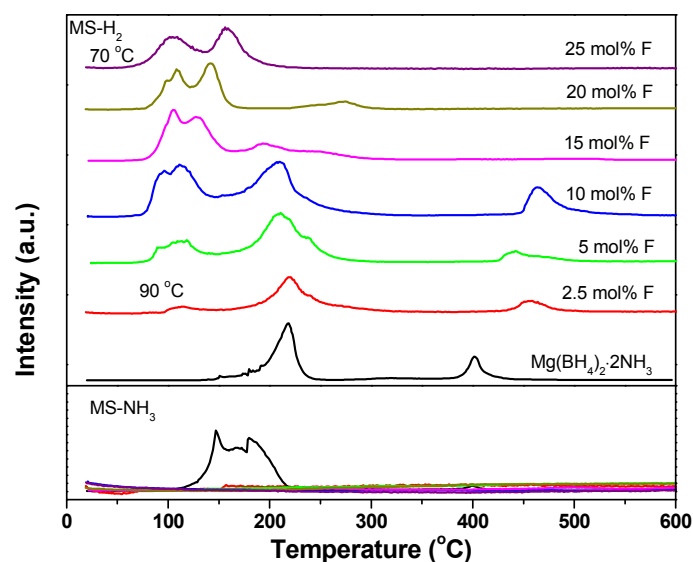


Fig. 3. TPD-MS curves of the F-substituted  $\text{Mg}(\text{BH}_4)_2 \cdot 2\text{NH}_3$ .

To evaluate the dehydrogenation behaviour quantitatively, the volumetric release curves of the F-substituted  $\text{Mg}(\text{BH}_4)_2 \cdot 2\text{NH}_3$  samples were measured and are shown in Fig. 4. As reported previously,<sup>26</sup> the pristine  $\text{Mg}(\text{BH}_4)_2 \cdot 2\text{NH}_3$  starts to evolve hydrogen at approximately 140  $^\circ\text{C}$ , amounting to approximately 14.8 wt% at 600  $^\circ\text{C}$ . After F-substitution, the onset dehydrogenation temperatures were lowered to below 90  $^\circ\text{C}$ . Hydrogen desorption amounting to 14.95, 14.40, 12.46, 11.20, 9.71 and 8.67 wt% was observed for the samples with F-substitution content of 2.5, 5, 10, 15, 20 and 25 mol%, respectively. The total dehydrogenation amount of F-substituted  $\text{Mg}(\text{BH}_4)_2 \cdot 2\text{NH}_3$  was gradually decreased with the

increase in the content of  $\text{LiBF}_4$  because  $\text{LiBF}_4$  does not contribute to hydrogen content. On the contrary, the dehydrogenation amount of the 2.5 mol% F-substituted  $\text{Mg}(\text{BH}_4)_2 \cdot 2\text{NH}_3$  was slightly larger than the dehydrogenation amount of the pristine ammoniate. Such a phenomenon may be attributed mainly to the depressed  $\text{NH}_3$  evolution due to F-substitution, which results in an increase in the dehydrogenation amount. Moreover, taking into consideration the amounts of hydrogen released during ball milling, the total dehydrogenation amounts were calculated to be 15.88, 16.00, 15.96, 15.90, 16.00 and 15.96 wt% for the samples with F-substitution content of 2.5, 5, 10, 15, 20 and 25 mol%, respectively, when excluding the  $\text{LiBF}_4$  amounts. These results are in excellent consonance with the theoretical hydrogen capacity of 16.03 wt% for  $\text{Mg}(\text{BH}_4)_2 \cdot 2\text{NH}_3$  and higher than the dehydrogenation amount of pristine  $\text{Mg}(\text{BH}_4)_2 \cdot 2\text{NH}_3$ . This observation quantitatively confirms the increase in hydrogen release due to the effective depression of  $\text{NH}_3$  evolution after F-substitution.

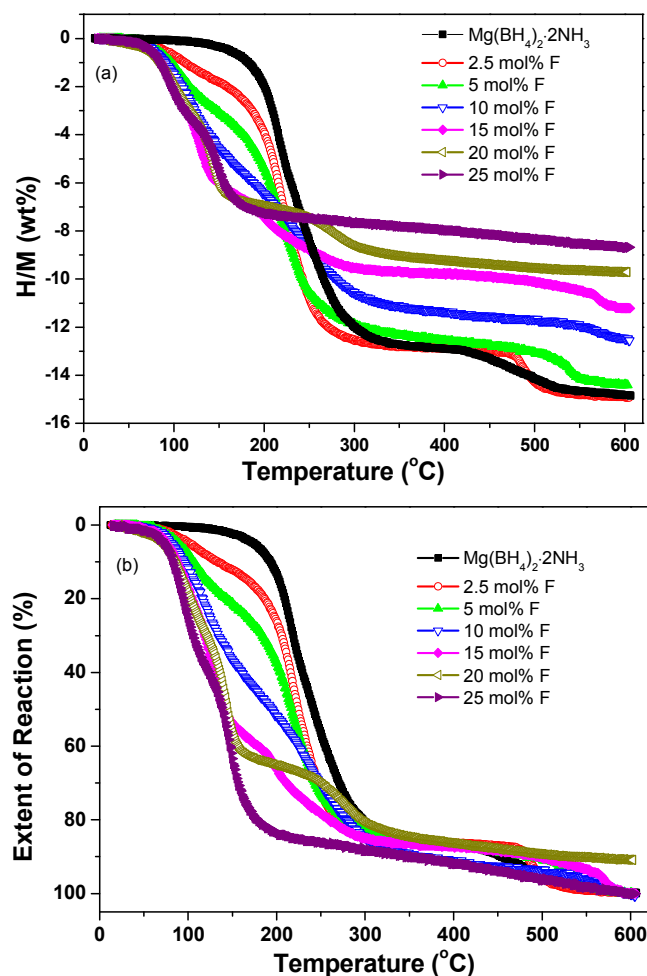


Fig. 4. Volumetric release (a) and extent of reaction (b) curves of the F-substituted  $\text{Mg}(\text{BH}_4)_2 \cdot 2\text{NH}_3$ .

For the F-substituted  $\text{Mg}(\text{BH}_4)_2 \cdot 2\text{NH}_3$  samples, an appreciable low-temperature shift was found by increasing the

F-substitution content by plotting the extent of the reaction against temperature as shown in Fig. 4b. The 25 mol% F-substituted  $\text{Mg}(\text{BH}_4)_2 \cdot 2\text{NH}_3$  released 65% of its hydrogen capacity when heated to 150 °C. However, no appreciable hydrogen release was observed for the pristine ammoniate under the same conditions. The positive effect of F-substitution on decreasing the dehydrogenation operating temperatures was further confirmed by comparing the volumetric-release curves of the F-substituted  $\text{Mg}(\text{BH}_4)_2 \cdot 2\text{NH}_3$  with the volumetric-release curves of the newly designed  $\text{Mg}(\text{BH}_4)_2 \cdot 2\text{NH}_3$ - $\text{LiBH}_4$  system. As shown in Fig. S2,<sup>†</sup> the onset and terminal dehydrogenation temperatures of the  $\text{Mg}(\text{BH}_4)_2 \cdot 2\text{NH}_3$ - $\text{LiBH}_4$  system are nearly identical to the onset and terminal dehydrogenation temperatures of the pristine  $\text{Mg}(\text{BH}_4)_2 \cdot 2\text{NH}_3$ , although a part of the hydrogen release moved slightly to lower temperatures. This result indicates that the presence of  $\text{LiBH}_4$  does not distinctly change the thermal decomposition behaviour of  $\text{Mg}(\text{BH}_4)_2 \cdot 2\text{NH}_3$ . As the sole discrepancy is the  $\text{F}^{\delta-}$  anion of  $\text{LiBF}_4$  in comparison with  $\text{LiBH}_4$ , we believe that the significantly improved dehydrogenation properties of the  $\text{Mg}(\text{BH}_4)_2 \cdot 2\text{NH}_3$ - $\text{LiBF}_4$  system originate from the substitution of F for H.

The effect of F-substitution on the isothermal dehydrogenation kinetics of  $\text{Mg}(\text{BH}_4)_2 \cdot 2\text{NH}_3$  was further elucidated by taking the 15 mol% F-substituted  $\text{Mg}(\text{BH}_4)_2 \cdot 2\text{NH}_3$  sample released more than 4 wt% of hydrogen within 100 min at 120 °C. When the dehydrogenation was conducted at 150 °C, hydrogen desorption from the 15 mol% F-substituted  $\text{Mg}(\text{BH}_4)_2 \cdot 2\text{NH}_3$  resulted in more than 5.2 wt% within only 40 min, whereas only 1.2 wt% was observed for the pristine sample. By analysing the tangent slope of the initial dehydrogenation stage, the rate constant of the 15 mol% F-substituted  $\text{Mg}(\text{BH}_4)_2 \cdot 2\text{NH}_3$  was determined to be 0.33 wt%·min<sup>-1</sup> at 120 °C, which is 20.6 times the pristine sample (0.016 wt%·min<sup>-1</sup>). Moreover, the dehydrogenation rate of the 15 mol% F-substituted  $\text{Mg}(\text{BH}_4)_2 \cdot 2\text{NH}_3$  at 150 °C (0.60 wt%·min<sup>-1</sup>) was 7.45 times faster than the pristine sample (0.071 wt%·min<sup>-1</sup>). Obviously, the F-substituted  $\text{Mg}(\text{BH}_4)_2 \cdot 2\text{NH}_3$  exhibits superior dehydrogenation kinetics to the pristine ammoniate.

To understand the reasons behind the improved dehydrogenation properties of the F-substituted  $\text{Mg}(\text{BH}_4)_2 \cdot 2\text{NH}_3$ , the 25 mol% F-substituted sample was selected as an example to analyse the heat flow information and structural changes during dehydrogenation. For the 25 mol% F-substituted  $\text{Mg}(\text{BH}_4)_2 \cdot 2\text{NH}_3$ , the  $[\text{BH}_4]^-$  anions were converted to new anions with the nominal composition of  $[\text{BH}_3\text{F}]^-$ . Fig. 6 demonstrates the DSC curves of the 25 mol% F-substituted  $\text{Mg}(\text{BH}_4)_2 \cdot 2\text{NH}_3$ . Four thermal events in the DSC curve of the pristine  $\text{Mg}(\text{BH}_4)_2 \cdot 2\text{NH}_3$  were observed in the testing temperature range (30 - 550 °C). A sharp endothermic peak is followed by an exothermic peak and two other endothermic peaks. According to the previous report,<sup>42</sup> the first endothermic peak should originate from the minor ammonia-release process of  $\text{Mg}(\text{BH}_4)_2 \cdot 2\text{NH}_3$ , and the other three heat flow peaks are all

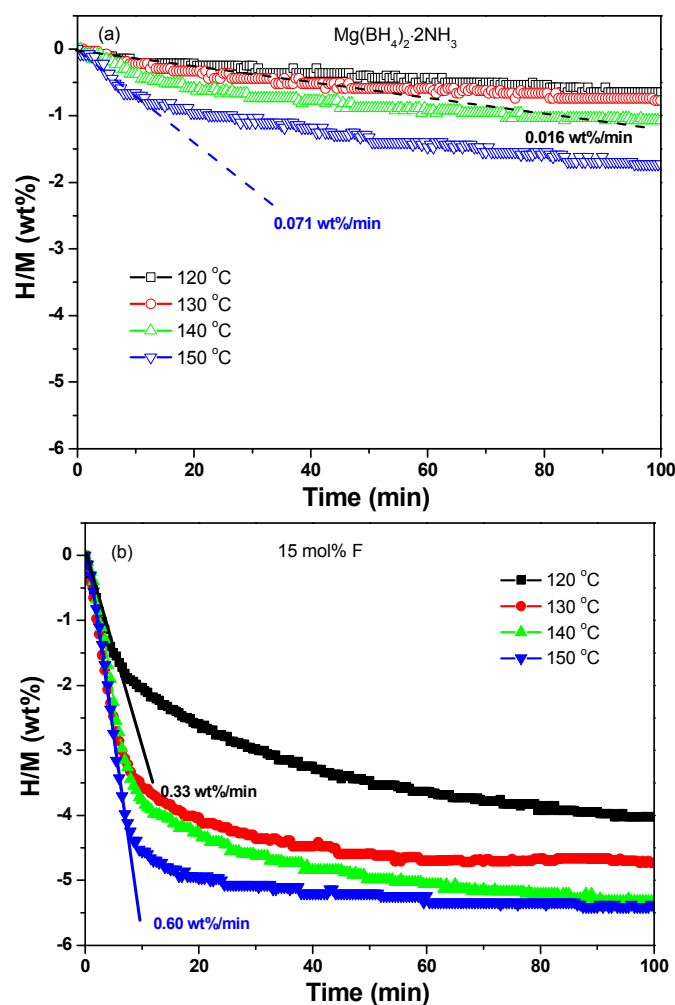


Fig. 5. Isothermal dehydrogenation curves for the pristine and 15 mol% F-substituted  $\text{Mg}(\text{BH}_4)_2 \cdot 2\text{NH}_3$ .

attributed to hydrogen release. Interestingly, only a broad exothermic signal peaked at 155 °C with a shoulder near 120 °C was detected with the disappearance of other heat flow peaks for the 25 mol% F-substituted  $\text{Mg}(\text{BH}_4)_2 \cdot 2\text{NH}_3$ . Specifically, the absence of endothermic events originating from the breakdown of Mg-N bonds matches well with the depressed  $\text{NH}_3$  evolution during the dehydrogenation of F-substituted  $\text{Mg}(\text{BH}_4)_2 \cdot 2\text{NH}_3$ . Combined with the TPD-MS results in Fig. 3, the exothermic event corresponds to hydrogen release, which appears at much lower temperatures than in the pristine  $\text{Mg}(\text{BH}_4)_2 \cdot 2\text{NH}_3$ , suggesting that there is a more favourable combination for  $\text{H}^{\delta+}$  and  $\text{H}^{\delta-}$  with the presence of F in  $[\text{BH}_4]^-$  anions. However, no appreciable changes in the heat flow behaviour were found for the  $\text{MgF}_2$ - and  $\text{LiBH}_4$ -added samples, which possess the same F and Li contents as the 25 mol% F-substituted  $\text{Mg}(\text{BH}_4)_2 \cdot 2\text{NH}_3$ , in comparison with the pristine  $\text{Mg}(\text{BH}_4)_2 \cdot 2\text{NH}_3$ . This fact further confirms the effectiveness of F-substitution for H in  $[\text{BH}_4]^-$  anions through the interactions between the  $[\text{BH}_4]^-$  and  $[\text{BF}_4]^-$  anions.

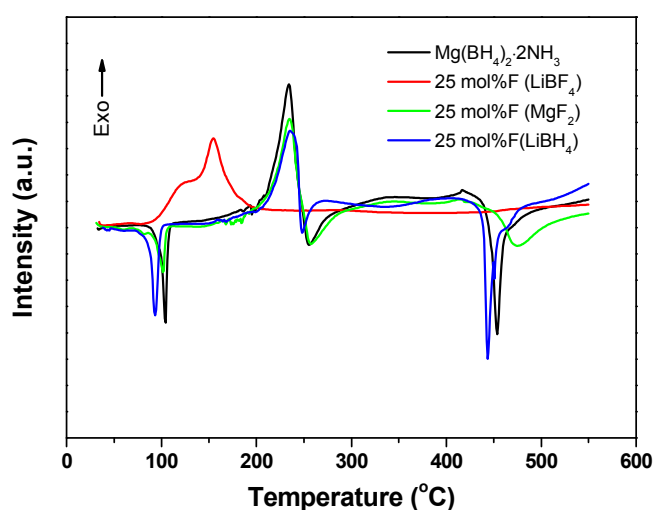


Fig. 6. DSC curves of the  $\text{Mg}(\text{BH}_4)_2 \cdot 2\text{NH}_3$  with different additives.

Fig. 7 presents the XRD patterns of the decomposition products of the 25 mol% F-substituted  $\text{Mg}(\text{BH}_4)_2 \cdot 2\text{NH}_3$  at different stages. As shown in Fig. 3, the first and second dehydrogenation peaks of the 25 mol% F-substituted  $\text{Mg}(\text{BH}_4)_2 \cdot 2\text{NH}_3$  overlapped with each other. Therefore, to obtain the first-step dehydrogenation product, the sample was heated to 100 °C and then maintained there for a sufficient amount of time. The completion of the first-step dehydrogenation was confirmed as no dehydrogenation signal was detected below 150 °C in the TPD-MS curve of the dehydrogenation product at 100 °C (Fig. S3†). As shown in Fig. 7, after dehydrogenation at 100 and 200 °C, only several weak and broad diffraction peaks from  $\text{MgF}_2$  were identified at 27.27, 40.42, 53.52, and 68.15° (2 $\theta$ ) with the disappearance of the sharp peaks of  $\text{MgLi}_{2/3}(\text{BH}_3\text{F})_{8/3} \cdot 2\text{NH}_3$ . Upon further heating the sample to 600 °C, the typical diffraction peaks of  $\text{MgF}_2$  and  $\text{LiF}$  dominated the XRD profile of the dehydrogenated product.

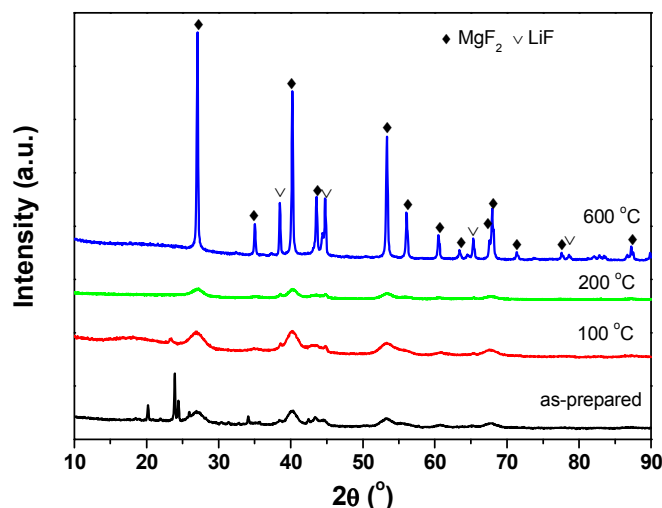


Fig. 7. XRD patterns of the 25 mol% F-substituted  $\text{Mg}(\text{BH}_4)_2 \cdot 2\text{NH}_3$  dehydrogenated at different stages.

Fig. 8 shows the FTIR spectra of the 25 mol% F-substituted  $\text{Mg}(\text{BH}_4)_2 \cdot 2\text{NH}_3$  dehydrogenated at different stages. For the sample dehydrogenated at 100 °C, the FTIR result indicated the existence of N-H and B-H stretching bands in the wavenumber range of 3400-3100  $\text{cm}^{-1}$  and 2500-2000  $\text{cm}^{-1}$ , respectively. At the same time, an appreciable change in the B-H bending modes was also observed, as the absorbance peaks in the wavenumber range of 1000-1300  $\text{cm}^{-1}$  merged into one broad signal peaking at approximately 1199  $\text{cm}^{-1}$ . In addition, a new B-N absorbance at 1441  $\text{cm}^{-1}$  with a higher relative intensity is also discernible in comparison with the peak at 1383  $\text{cm}^{-1}$  in the as-prepared sample, suggesting the formation of novel compounds containing B-N bonds. These results further indicate that the first-step dehydrogenation should originate mainly from the local combination of  $\text{H}^{\delta-}$  in  $[\text{BH}_3\text{F}]^-$  anions and  $\text{H}^{\delta+}$  in  $\text{NH}_3$  groups, which gives rise to B-N bond formation.

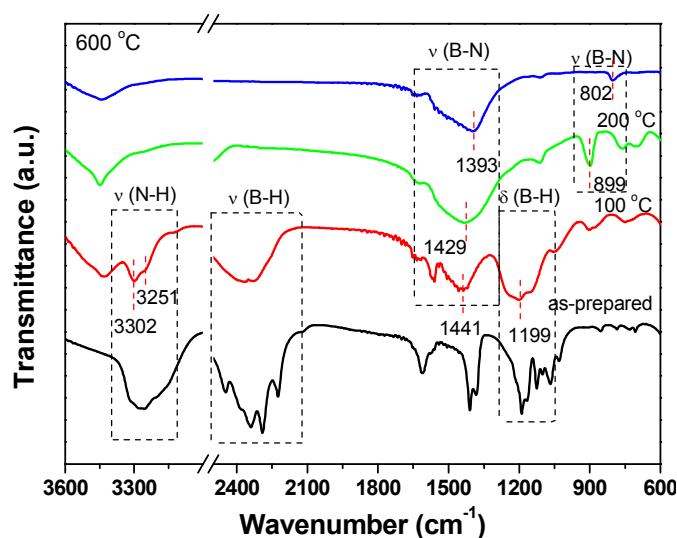
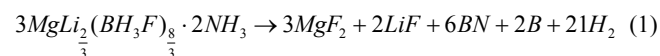


Fig. 8 FTIR spectra of the 25 mol% F-substituted  $\text{Mg}(\text{BH}_4)_2 \cdot 2\text{NH}_3$  dehydrogenated at different stages.

After dehydrogenation at 200 °C, the absorbance of B-N bonding was intensified with a red-shift to 1429  $\text{cm}^{-1}$ . However, the N-H stretching bands in 3500-3000  $\text{cm}^{-1}$ , B-H stretching bands in 2500-2000  $\text{cm}^{-1}$  and B-H bending bands in 1400-1000  $\text{cm}^{-1}$  disappeared, indicating the complete consumption of the B-H and N-H bonds. These findings further reveal that the hydrogen release of the F-substituted  $\text{Mg}(\text{BH}_4)_2 \cdot 2\text{NH}_3$  is most likely driven by the combination of  $\text{H}^{\delta+}$  in  $\text{NH}_3$  and  $\text{H}^{\delta-}$  in  $[\text{BH}_3\text{F}]^-$ , which consumes the B-H and N-H bonds and generates the BN compound. In addition, there is still a small amount of H bonded because the B-N absorbance appears at 1429  $\text{cm}^{-1}$ , as reported previously.<sup>25</sup> When the 25 mol% F-substituted  $\text{Mg}(\text{BH}_4)_2 \cdot 2\text{NH}_3$  was heated to 600 °C, only two absorbance peaks at 1393 and 802  $\text{cm}^{-1}$  were observed in the testing wavenumber range, which can be attributed to the B-N bonds in boron nitride (BN).<sup>43</sup>

Combining XRD and FTIR analyses, we conclude that upon heating, the F-substituted  $\text{Mg}(\text{BH}_4)_2 \cdot 2\text{NH}_3$  liberated hydrogen by the interaction between  $\text{H}^{\delta+}$  and  $\text{H}^{\delta-}$  to convert to  $\text{MgF}_2$ , LiF

and BN. Moreover, boron is also likely to be involved in the final decomposition product because the nominal composition of the 25 mol% F-substituted  $\text{Mg}(\text{BH}_4)_2 \cdot 2\text{NH}_3$  is  $\text{MgLi}_{2/3}(\text{BH}_3\text{F})_{8/3} \cdot 2\text{NH}_3$ . In summary, the overall decomposition process of the 25 mol% F-substituted  $\text{Mg}(\text{BH}_4)_2 \cdot 2\text{NH}_3$  can be described as reaction (1). Hydrogen release in reaction (1) amounts to 9.37 wt%, which is in good agreement with the experimental result (9.21 wt%). Such a hydrogen capacity is quite high and sufficient for hydrogen storage applications.



As mentioned above, a blue shift of the B-H vibration, which represents the strengthened B-H bonds in the F-substituted  $\text{Mg}(\text{BH}_4)_2 \cdot 2\text{NH}_3$ , occurred after F-substitution. The bonding energy of the B-H bond was increased after F substitution. The polarity of a covalent bond is known to be closely related to the bond energy: the higher the bond energy, the higher the polarity of the covalent bond. As a consequence, the  $\text{H}^{\delta-}$  in  $[\text{BH}_4]^-$  anions of the F-substituted  $\text{Mg}(\text{BH}_4)_2 \cdot 2\text{NH}_3$  are more negative than the  $\text{H}^{\delta-}$  in the pristine sample. This property should facilitate the combination of  $\text{H}^{\delta+}$  and  $\text{H}^{\delta-}$  for hydrogen release as its driving force originates from the electrostatic interaction between  $\text{H}^{\delta-}$  and  $\text{H}^{\delta+}$ . In addition, there are two competing processes during the decomposition of  $\text{Mg}(\text{BH}_4)_2 \cdot 2\text{NH}_3$ : hydrogen desorption driven by the local combination of  $\text{H}^{\delta+}$  and  $\text{H}^{\delta-}$  and ammonia evolution caused by the breakdown of Mg-N bonds.<sup>26</sup> Thus, the preferred  $\text{H}^{\delta-}\text{-H}^{\delta+}$  combination in F-substituted  $\text{Mg}(\text{BH}_4)_2 \cdot 2\text{NH}_3$  consumes the  $\text{NH}_3$  groups preferentially. This effect may explain the remarkably depressed ammonia release.

To further evaluate the mechanisms of F-substitution in improving the dehydrogenation properties of  $\text{Mg}(\text{BH}_4)_2 \cdot 2\text{NH}_3$ , TPD-MS and TG measurements were conducted on the  $\text{Mg}(\text{BH}_4)_2 \cdot (2/3)\text{LiBF}_4$  system (25 mol% F-substituted  $\text{Mg}(\text{BH}_4)_2$ ). As shown in Fig. 9,  $\text{B}_2\text{H}_6$  is evidently detected in the temperature range of 100-175 °C for F-substituted  $\text{Mg}(\text{BH}_4)_2$ , whereas hydrogen is the sole gaseous product when heating the pristine  $\text{Mg}(\text{BH}_4)_2$ . In addition, combining the volumetric-release and TG results (Fig. S4†), the  $\text{H}_2$  to  $\text{B}_2\text{H}_6$  molar ratio was determined to be 1:1 for the F-substituted  $\text{Mg}(\text{BH}_4)_2$ , indicating a substantial amount of diborane release. A similar phenomenon was also discovered in the decomposition of  $\text{Al}(\text{BH}_4)_3$  and some transition metal borohydrides.<sup>44-46</sup> These results suggest that the Mg-B bond in  $\text{Mg}(\text{BH}_4)_2$  was weakened after F-substitution. As a consequence, we believe that the Mg-B bonds in  $\text{Mg}(\text{BH}_4)_2 \cdot 2\text{NH}_3$  were also weakened after F-substitution, when the bonds are more readily broken, thus favouring the generation of B-N bonds during the thermal decomposition. The  $\text{NH}_3$  is known to serve as a “stabilising agent” to stabilise the aluminium borohydride and transition metal borohydrides with the formation of corresponding ammoniates.<sup>45,47</sup> In this case, the  $\text{NH}_3$  groups in the F-substituted  $\text{Mg}(\text{BH}_4)_2 \cdot 2\text{NH}_3$  should play a similar role. Thus, the weakened Mg-B bonds and

the higher magnitude of charge on the  $H^{\delta-}$  are reasonably responsible for the improved dehydrogenation properties of F-substituted  $Mg(BH_4)_2 \cdot 2NH_3$ .

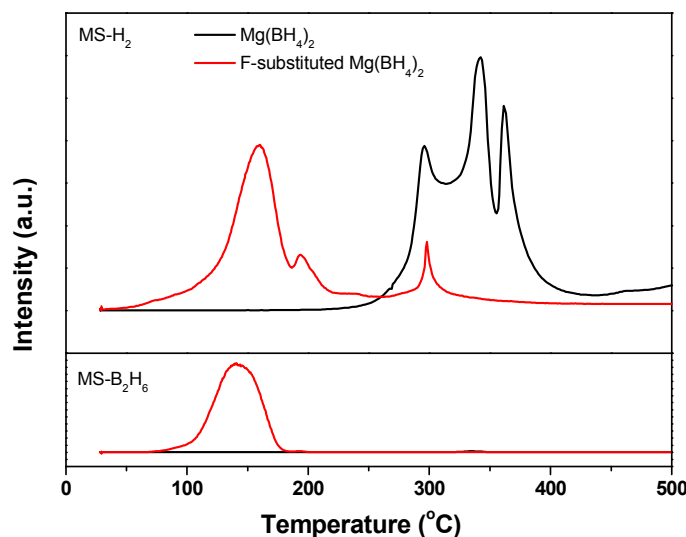


Fig. 9. TPD-MS curves of the F-substituted  $Mg(BH_4)_2$ .

The fully dehydrogenated product was subjected to hydrogenation at 500 °C with an initial hydrogen pressure of 100 bar. However, hydrogen desorption from the F-substituted  $Mg(BH_4)_2 \cdot 2NH_3$  is exothermic in nature (Fig. 6), and no hydrogen uptake was observed under the present conditions. Therefore, further modification of the thermodynamics should be conducted to achieve reversible hydrogen storage.

## Conclusions

In this work, a F-substituted  $Mg(BH_4)_2 \cdot 2NH_3$  was synthesised by ball milling  $Mg(BH_4)_2 \cdot 2NH_3$  with  $LiBF_4$  based on the interaction between  $[BH_4]^-$  and  $[BF_4]^-$  anions. The operating temperatures for hydrogen desorption from  $Mg(BH_4)_2 \cdot 2NH_3$  were determined to be remarkably reduced, and the evolution of  $NH_3$  was effectively depressed after F-substitution. The onset dehydrogenation temperature of the 25 mol% F-substituted  $Mg(BH_4)_2 \cdot 2NH_3$  samples was only approximately 70 °C, which is decreased by 80 °C in comparison with the pristine  $Mg(BH_4)_2 \cdot 2NH_3$ . During the heating of the 25 mol% F-substituted  $Mg(BH_4)_2 \cdot 2NH_3$  to 150 °C, approximately 65% of the hydrogen capacity was released. However, no appreciable hydrogen release was observed for the pristine sample under the same conditions. Structure analyses revealed a blue shift for the B-H vibration after F-substitution, representing the strengthening of the B-H bonds. The strengthened B-H bonds offered a higher magnitude of charge on  $H^{\delta-}$ , which facilitated the combination of  $H^{\delta+}$  and  $H^{\delta-}$  for hydrogen release and accordingly depressed the ammonia release. Conversely, the F-substitution weakened the Mg-B bonds in  $Mg(BH_4)_2 \cdot 2NH_3$ , which thus facilitated the formation of BN during dehydrogenation. Both the increased magnitude of charge on  $H^{\delta-}$  and the decreased strength of Mg-B bonds contribute to the

improved dehydrogenation properties of F-substituted  $Mg(BH_4)_2 \cdot 2NH_3$ . However, no hydrogen uptake was detected at 500 °C and 100 bar of hydrogen pressure for the fully dehydrogenated product. Therefore, further thermodynamic modification is warranted to achieve reversible hydrogen storage.

## Acknowledgments

We gratefully acknowledge financial support received from the National Natural Science Foundation of China (51171170, 51222101, 51025102), the Research Fund for the Doctoral Program of Higher Education of China (20130101110080, 20130101130007), the Program for Innovative Research Team in the University of Ministry of Education of China (IRT13037), and the Fundamental Research Funds for the Central Universities (2014XZZX003-08).

## Notes

<sup>a</sup>State Key Laboratory of Silicon Materials, Key Laboratory of Advanced Materials and Applications for Batteries of Zhejiang Province and Department of Materials Science and Engineering, Zhejiang University, Hangzhou 310027, China. E-mail: [mselyf@zju.edu.cn](mailto:mselyf@zju.edu.cn) (Y.F.L.), [hghan@zju.edu.cn](mailto:hghan@zju.edu.cn) (H.G.P.); Fax: +86 571 87952615; Tel: +86 571 87952615

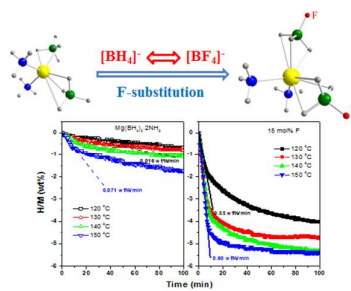
<sup>b</sup>Science and Technology on Combustion and Explosion Laboratory, Xi'an Modern Chemistry Research Institute, Xi'an 710065, China

†Electronic Supplementary Information (ESI) available: FTIR spectra of  $Mg(BH_4)_2 \cdot 2NH_3$ - $MgF_2$ , Volumetric release curves of  $Mg(BH_4)_2 \cdot 2NH_3$ - $LiBH_4$ , MS curves of 25 mol% F-doped  $Mg(BH_4)_2 \cdot 2NH_3$  and its decomposition product, Volumetric-release and TG curves of F-substituted  $Mg(BH_4)_2$ . See DOI: 10.1039/b000000x/

## References

- I. Jain, *Int. J. Hydrogen Energy*, 2009, **34**, 7368-7378.
- M. Felderhoff, C. Weidenthaler, R. von Helmolt and U. Eberle, *Phys. Chem. Chem. Phys.*, 2007, **9**, 2643-2653.
- L. Schlapbach and A. Züttel, *Nature*, 2001, **414**, 353-358.
- S.-i. Orimo, Y. Nakamori, J. R. Eliseo, A. Züttel and C. M. Jensen, *Chem. Rev.*, 2007, **107**, 4111-4132.
- H.-W. Li, Y. Yan, S.-i. Orimo, A. Züttel and C. M. Jensen, *Energies*, 2011, **4**, 185-214.
- Z.-Z. Fang, X.-D. Kang, Z.-X. Yang, G. S. Walker and P. Wang, *J. Phys. Chem. C*, 2011, **115**, 11839-11845.
- J. E. Chen, Y. Zhang, Z. T. Xiong, G. T. Wu, H. L. Chu, T. He and P. Chen, *Int. J. Hydrogen Energy*, 2012, **37**, 12425-12431.
- E. G. Bardají, Z. Zhao-Karger, N. Boucharat, A. Nale, M. J. van Setten, W. Lohstroh, E. Röhm, M. Catti and M. Fichtner, *J. Phys. Chem. C*, 2011, **115**, 6095-6101.
- J. J. Vajo, S. L. Skeith and F. Mertens, *J. Phys. Chem. B*, 2005, **109**, 3719-3722.
- M. Fichtner, Z. Zhao-Karger, J. Hu, A. Roth and P. Weidler, *Nanotechnology*, 2009, **20**, 204029.
- Y. P. Pang, Y. F. Liu, M. X. Gao, L. Z. Ouyang, J. W. Liu, H. Wang, M. Zhu and H. G. Pan, *Nat. Commun.* 2014, **5**, 3519; Y. G. Yan, Y. S. Au, D. Rentsch, A. Remhof, P. E. de Jongh and A. Züttel, *J. Mater. Chem. A*, 2013, **1**, 11177-11183; J. M. Huang, Y. R. Yan, L.

- Z. Ouyang, H. Wang, J. W. Liu and M. Zhu, *Dalton Trans.*, 2014, **43**, 410-413.
- 12 L. H. Rude, E. Groppo, L. M. Arnbjerg, D. B. Ravnsbaek, R. A. Malmkjaer, Y. Filinchuk, M. Baricco, F. Besenbacher and T. R. Jensen, *J. Alloys Compd.*, 2011, **509**, 8299-8305.
- 13 E. A. Nickels, M. O. Jones, W. I. David, S. R. Johnson, R. L. Lowton, M. Sommariva and P. P. Edwards, *Angew. chem. Int. Edi.*, 2008, **47**, 2817-2819.
- 14 Z. Huang and T. Autrey, *Energy Environ. Sci.*, 2012, **5**, 9257-9268.
- 15 P. Wang, *Dalton Trans.*, 2012, **41**, 4296-4302.
- 16 K. Wang, J. G. Zhang, T. T. Man, M. Wu and C. C. Chen, *Chem. Asian J.*, 2013.
- 17 Z. T. Xiong, C. K. Yong, G. T. Wu, P. Chen, W. Shaw, A. Karkamkar, T. Autrey, M. O. Jones, S. R. Johnson and P. P. Edwards, *Nat. Mater.*, 2007, **7**, 138-141.
- 18 P. Chen, Z. T. Xiong, J. Z. Luo, J. Y. Lin and K. L. Tan, *Nature*, 2002, **420**, 302-304.
- 19 Z. T. Xiong, G. T. Wu, J. J. Hu and P. Chen, *Adv. Mater.*, 2004, **16**, 1522-1525.
- 20 Y. F. Liu, K. Zhong, K. Luo, M. X. Gao, H. G. Pan and Q. D. Wang, *J. Am. Chem. Soc.*, 2009, **131**, 1862-1870.
- 21 G. P. Meisner, M. L. Scullin, M. P. Balogh, F. E. Pinkerton and M. S. Meyer, *J. Phys. Chem. B*, 2006, **110**, 4186-4192.
- 22 X. Y. Chen, Y. H. Guo and X. B. Yu, *J. Phys. Chem. C*, 2010, **114**, 17947-17953.
- 23 W. W. Sun, X. W. Chen, Q. F. Gu, K. S. Wallwork, Y. B. Tan, Z. W. Tang and X. B. Yu, *Chem. Eur. J.*, 2012, **18**, 6825-6834;
- 24 Y. J. Yang, Y. F. Liu, Y. Li, M. X. Gao and H. G. Pan, *J. Phys. Chem. C*, 2013, **117**, 16326-16335; H. L. Chu, G. T. Wu, Z. T. Xiong, J. P. Guo, T. He and P. Chen, *Chem. Mater.*, 2010, **22**, 6021-6028; Y. H. Guo, Y. X. Jiang, G. L. Xia and X. B. Yu, *Chem. Commun.*, 2012, **48**, 4408-4410.
- 25 G. Soloveichik, J.-H. Her, P. W. Stephens, Y. Gao, J. Rijssenbeek, M. Andrus and J.-C. Zhao, *Inorg. Chem.*, 2008, **47**, 4290-4298.
- 26 Y. J. Yang, Y. F. Liu, Y. Li, M. X. Gao and H. G. Pan, *Chem. Asian J.*, 2013, **8**, 476-481.
- 27 Y. J. Yang, Y. F. Liu, H. Wu, W. Zhou, M. X. Gao and H. G. Pan, *Phys. Chem. Chem. Phys.*, 2014, **16**, 135-143.
- 28 Y. H. Guo, H. Wu, W. Zhou and X. B. Yu, *J. Am. Chem. Soc.*, 2011, **133**, 4690-4693.
- 29 L. C. Yin, P. Wang, Z. Z. Fang and H. M. Cheng, *Chem. Phys. Lett.*, 2008, **450**, 318-321.
- 30 M. Corno, E. Pinatel, P. Ugliengo and M. Baricco, *J. Alloys Compd.*, 2011, **509**, S679-S683.
- 31 I. Saldan, *Cent. Eur. J. Chem.*, 2011, **9**, 761-775.
- 32 H. I. Schlesinger, H. C. Brown, J. R. Gilbreath and J. J. Katz, *J. Am. Chem. Soc.*, 1953, **75**, 195-199.
- 33 H. C. Brown, *Hydroboration*, W. A. Benjamin, Inc., New York, 1962.
- 34 V. D. Aftandilian, H. C. Miller and E. L. Muetterties, *J. Am. Chem. Soc.*, 1961, **83**, 2471-2474.
- 35 A. Finch, P. J. Gardner and N. Hill, *J. Chem. Soc., Dalton Trans.*, 1975, 357-359.
- 36 E. Baughan, in *Coordinative Interactions*, Springer, 1973, pp. 53-71.
- 37 R. H. Heyn, I. Saldan, M. H. Sørby, C. Frommen, B. Arstad, A. M. Bougza, H. Fjellvåg and B. C. Hauback, *Phys. Chem. Chem. Phys.*, 2013.
- 38 L. H. Rude, U. Filsø, V. D'Anna, A. Spyratou, B. Richter, S. Hino, O. Zavorotynska, M. Baricco, M. Sørby and B. Hauback, *Phys. Chem. Chem. Phys.*, 2013, **15**, 18185-18194.
- 39 Y. F. Liu, Y. J. Yang, Y. F. Zhou, Y. Zhang, M. X. Gao and H. G. Pan, *Int. J. Hydrogen Energy*, 2012, **37**, 17137-17145.
- 40 P. A. Chater, W. I. David, S. R. Johnson, P. P. Edwards and P. A. Anderson, *Chem. Commun.*, 2006, 2439-2441.
- 41 E. L. Muetterties, J. H. Balthis, Y. T. Chia, W. H. Knoth and H. C. Miller, *Inorg. Chem.*, 1964, **3**, 444-451.
- 42 Y. J. Yang, Y. F. Liu, Y. Zhang, Y. Li, M. X. Gao and H. G. Pan, *J. Alloys Compd.*, 2014, **585**, 674-680.
- 43 D. P. Kim, K. T. Moon, J. G. Kho, J. Economy, C. Gervais and F. Babonneau, *Polym. Advan. Technol.*, 1999, **10**, 702-712.
- 44 T. J. Marks and J. R. Kolb, *Chem. Rev.*, 1977, **77**, 263-293.
- 45 Y. H. Guo, X. B. Yu, W. W. Sun, D. L. Sun and W. N. Yang, *Angew. chem. Int. Edi.*, 2011, **50**, 1087-1091.
- 46 O. Friedrichs, A. Remhof, A. Borgschulte, F. Buchter, S. Orimo and A. Züttel, *Phys. Chem. Chem. Phys.*, 2010, **12**, 10919-10922.
- 47 Z. W. Tang, F. Yuan, Q. F. Gu, Y. B. Tan, X. W. Chen, C. M. Jensen and X. B. Yu, *Acta Mater.*, 2013, **61**, 3110-3119.

**Graphical contents entry:**

Fluorine-substituted Mg(BH<sub>4</sub>)<sub>2</sub>·2NH<sub>3</sub> possesses significantly improved dehydrogenation properties.